Thermodynamic optimization of solar aided liquid air energy storage systems

Katski, Bartosz G.; Desai, Nishith B.; Haglind, Fredrik

Published in:
Energy Proceedings

Link to article, DOI:
10.46855/energy-proceedings-11168

Publication date:
2024

Document Version
Publisher's PDF, also known as Version of record

Energy Proceedings
Vol 46, 2024
ISSN 2004-2965

Thermodynamic optimization of solar aided liquid air energy storage systems

Bartosz G. Kątski[1], Nishith B. Desai[1], Fredrik Haglind[1*]

1 Department of Civil and Mechanical Engineering, Technical University of Denmark, Kongens Lyngby, Denmark (*fhag@dtu.dk)

ABSTRACT

Liquid air energy storage is a promising large-scale energy storage technology with high energy density for increasingly weather-dependent power grids, with no geographical constraints. The round-trip efficiency of a standalone liquid air energy storage system is predicted to be between 40 % and 67 %. An attractive way to increase the economic viability of the liquid air energy storage system is to couple the system with additional heat sources. Incorporating concentrated solar power has recently been proposed to increase the temperature at the inlet of the air turbines, and thus boosting the discharging power output and round-trip efficiency. This paper aims to find the optimal system design based on concentrated solar power temperature, considering both energy storage and power production metrics. The analyzed liquid air energy storage system is based on the Linde cycle, two tank thermal oil system for compression heat storage, and a two tank, two stage cold recovery system using methanol and liquid propane. A heliostat system with two-tank direct molten salt thermal energy storage is used as an additional heat source. A supercritical organic Rankine cycle system is used for excess heat recovery with R32 as working fluid. Novel ways of integrating the organic Rankine cycle system for multiple-source excess heat utilization were analyzed. Effects of charging and discharging pressures, number of air compressors and turbines and solar heat transfer fluid temperatures on the optimal organic Rankine cycle design and round-trip exergy ratio were studied. The results suggest that a maximum round-trip exergy ratio of 62.2 % can be achieved. The paper provides a basis for further optimization of design and operation of the solar aided liquid air energy storage systems, especially in off-design conditions for low sun availability.

Keywords: energy storage, solar aided liquid air energy storage, concentrated solar power, organic Rankine cycle

NOMENCLATURE

Abbreviations	
AR	Air regenerator
ARC	Absorption refrigeration cycle
CRS	Central receiver system
CSP	Concentrated solar power
DH	District heating
DHW	Domestic hot water
HTF	Heat transfer fluid
LAES	Liquid air energy storage
ORC	Organic Rankine cycle
PTSC	Parabolic trough solar collector
SALAES	Solar aided liquid air energy storage
STC	Solar thermal collector
TEG	Thermoelectric generator
Symbols	
Ex	Exergy (MWh)
h	Specific enthalpy (kJ/kgK)
$\dot{m}$	Mass flow rate (kg/s)
Q	Heat (MWh_{th})
RTE_{ex}	Round trip exergy ratio (-)
RTE	Round trip efficiency (-)
t	Time (s)
W	Work (MWh)
$\dot{W}$	Power (kW)
Y	Liquid yield (-)
η_{sol}	Solar power cycle efficiency (-)
η_{is}	Isentropic efficiency (-)
η_{ORC}	Organic Rankine cycle thermal efficiency (-)
Subscripts	
AC	Air compressor
AT	Air turbine
ch	Charge cycle
CRP	Air cryo-pump
CRT	Air cryo-turbine
dis	Discharge cycle
evap	Evaporation
in	Inlet
is	Isentropic
OP	Organic Rankine cycle pump
OT	Organic Rankine cycle turbine
out	Outlet
salt	Solar molten salt
Other subscripts refer to stream numbers on Fig. 1	

This is a paper for 15th International Conference on Applied Energy (ICAE2023), Dec. 3-7, 2023, Doha, Qatar.

1. INTRODUCTION

In order to meet the carbon neutrality goals [1], the energy sector in Europe is now under transformation. Between the years 2011 and 2021 the share of solar and wind power increased from 2 % to 10 % of global production [2]. Growing penetration of weather-dependent electricity sources leads to electric grid instability. The way to mitigate the changes is the introduction of short, medium, and long duration energy storage [3].

Liquid air energy storage (LAES) is one of the promising technologies that are proposed for medium duration energy storage (4h – 200h [4]). The round-trip efficiency (RTE) is predicted to be between 40 % and 67 % [4]. A way to increase the economic attractiveness of the system is integration with external hot or cold energy sources [6]. Coupling with concentrated solar power (CSP) is deemed especially beneficial for sun-rich regions. Several articles have been published investigating solar aided LAES (SALAES) systems. However, there is a vast diversity in operation parameters and the design of the systems in the literature (see Table 1).

Several authors proposed using one working fluid for both compression intercooling and solar heat collection [7, 8]. This approach reduces the excess heat sources; however, it can also limit the temperature range in the solar receiver. Another design strategy is to only use solar heat directly for the air turbines, and to utilize all compression heat to run an organic Rankine cycle (ORC) unit [9] or to supply hot water [10-12]. Yang et al. [8] proposed isothermal compression, and stated that the exergy efficiency increased significantly, especially for layouts with higher number of compressors and turbines, due to low amounts of excess heat. Zhou et al. [13] reported that using both compression heat and solar heat directly for the air turbines (as shown on Fig. 1) increases the exergy efficiency by 3.7 % compared to using compression heat only in an ORC unit. A similar system was proposed by Ding [14]. This approach enables storage operation during low sun availability (in off-design conditions and with penalty on turbine efficiency).

Introducing an additional heat source (e.g., CSP) may lead to a significant limitation of compression heat utilization directly for the air turbines during discharge, especially for high temperature additional heat sources. This relation enhances the role of excess heat utilization. Moreover, increasing the solar heat transfer fluid (HTF) temperature increases the turbine outlet temperature (for a constant pressure ratio). The thermal oil returning from the inter-heaters is thus hotter and a new source of valuable heat is available. The excess heat utilization methods used in the literature are listed in Table 1. Air regeneration occurs in most of the proposed systems, and it uses the hot air from the outlet of the last turbine to preheat the air coming out from the evaporators. In other systems, the turbine outlet air is expelled to the atmosphere [14] or used in the ORC preheater [13, 15, 16]. Ebrahimi [17] used compression heat to run a Kalina cogeneration cycle. Li et al. [7] suggested using compression heat in the ORC unit during charging, and the same ORC unit to cool down the solar-heated oil after the inter-heaters during discharge. Ding et al. [14] proposed to use two separate ORC systems to exploit these two sources simultaneously. Running a single ORC unit using both high and lower grade heat concurrently has not yet been proposed.

This paper aims to find the optimal system design based on concentrated solar power temperature, considering both energy storage and power production

Table 1 Main parameters of SALAES systems in the literature.

Ref.	CSP type	Solar HTF	HTF max temp. [K]	Turbine inlet max temp. [K]	Charge pressure [bar]	Discharge pressure [bar]	No of compressors	No of turbines	Mean comp. ratio	Mean exp. ratio	Excess heat utilization
[7]	PTSC	Oil	NA	565.5	160.0	120.0	3	3	5.4	4.9	AR, ORC (coupling charge and discharge), ARC
[8]	PTSC	Oil	623.2	NA	137.2	91.8	3	3	5.2	4.5	AR
[8]	PTSC	Oil	623.2	NA	137.2	91.8	4	4	3.4	3.1	AR
[8]	PTSC	Oil	623.2	NA	137.2	91.8	5	5	2.7	2.5	AR
[9]	CRS	Salt	823.2	818.2	160.0	120.0	3	3	5.4	4.9	AR, ORC, DHW
[10]	CRS	Salt	823.2	818.2	160.0	120.0	3	3	5.4	4.9	AR, DH, DHW
[11]	STC	Oil	NA	608.2	NA	NA	4	1	NA	NA	NA
[12]	CRS	Salt	1373.2	1363.2	150.0	90.0	3	1	5.3	90.0	AR, ORC
[13,15,16]	PTSC	Salt	673.2	593.2	155.0	70.0	4	3	3.5	4.1	ORC, TEG
[14]	PTSC	Oil	553.2	493.2	110.0	51.3	4	3	3.2	3.7	2 ORC units
[17]	PTSC	Oil	573.2	567.2	66.5	88.5	2	3	8.2	4.5	AR, Kalina cogeneration
[18]	PTSC	Oil	~650	NA	203.9	94.7	2	3	14.3	4.6	AR, CSP steam cycle
[19]	PTSC	Oil	603.9	593.9	NA	39.0	NA	3	NA	13 / 3	AR

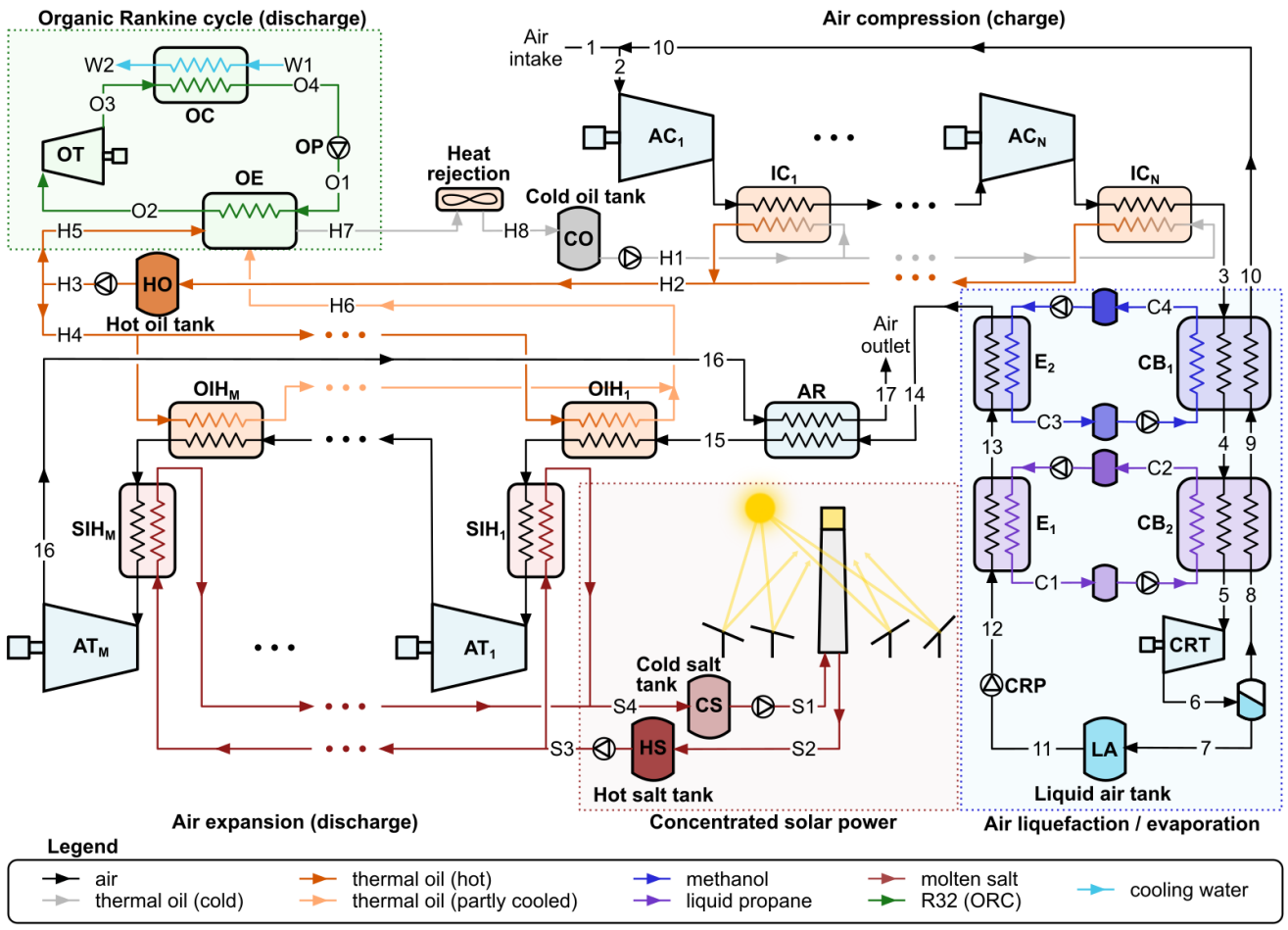

Fig. 1 Simplified schematic of the proposed SALAES system

metrics. The analyzed LAES system is based on the Linde cycle, two tank thermal oil system for compression heat storage, and a two tank, two stage cold recovery system using methanol and liquid propane. A heliostat system with two-tank direct molten salt thermal energy storage is used as an additional heat source. A supercritical organic Rankine cycle system is used for excess heat recovery with R32 as working fluid. Novel ways of integrating the organic Rankine cycle system using both the high and lower grade heat were analyzed. Effects of charging and discharging pressures, number of air compressors and turbines and solar heat transfer fluid temperatures on the optimal ORC design and round-trip exergy ratio were studied.

The main novelties of this paper are the new configurations of ORC evaporator (improvement of system similar to the ones proposed by Zhou et al. [13] and Ding et al. [14]) and the optimization of SALAES system design with two separate fluids for compression intercooling and solar heat collection (as opposed to study by Yang et al. [9] who only used one fluid for similar optimization) also studying the effects of solar heat temperatures on the optimal design.

2. SYSTEM DESCRIPTION

2.1 Charging

A simplified schematic of the proposed system is shown in Fig. 1. During the charging process the air from the atmosphere (state 1) is compressed to high pressures (from state 2 to state 3) using a number of compressors (AC). In order to decrease the power input, the air is intercooled (IC) using thermal oil from the cold oil tank (CO). Extracted heat is then stored in hot oil tank (HO). Next, the pressurized air is cooled down (from state 3 to state 5) using cold liquid methanol (CB_1) and liquid propane (CB_2). After that, the cryogenic air enters the cryo-turbine (CRT) and is expanded into the two-phase region (state 6). The liquid phase is separated and put in a tank at ambient pressure (LA) at 78.9 K. The gaseous phase is returned to the cold-box (CB_1, CB_2) (state 8 to state 10) where it takes part in cooling down the high-pressure air, and is then mixed with the intake air.

2.2 Discharging

During discharge, the liquid air is pumped to a high pressure (from state 11 to state 12) using the cryo-pump

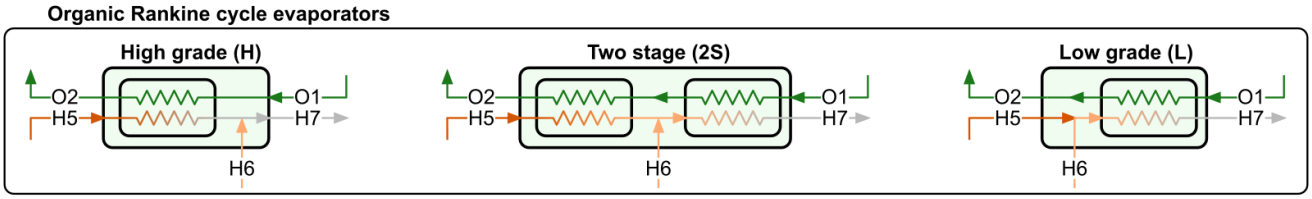

Fig. 2 Configurations of ORC evaporator (OE)

(CRP) and is then evaporated (state 12 to state 14). Cold thermal energy is extracted from air by the cold fluids (E_1, E_2) and is stored for the next liquefaction process (charging). The air is further heated up (from state 14 to state 15) in the regenerator (AR) to utilize excess energy from the outlet of the last turbine (AT_M).

2.2.1 Standard LAES system

In a standalone LAES, the preheated air is brought to high temperatures by hot thermal oil (OIH) which stores compression heat from the charging process (HO). Air is then expanded in turbines (AT) with intermediate heating.

2.2.2 Solar aided LAES system (SALAES)

By connecting solar power to a LAES, the turbine (AT) inlet temperature can be increased, thereby raising the power cycle thermal efficiency. Molten salt is heated up in the solar receiver and is then stored in the hot salt tank (HS). Throughout discharge, the hot salt is pumped to salt inter-heaters (SIH), significantly increasing the air temperature before the turbines. Depending on the temperature levels of the hot thermal oil and turbine outlet temperature, the oil inter-heaters (OIH) can work as preheaters or must be bypassed.

2.3 Excess heat utilization

There are three sources of excess heat in the proposed system.

1. The outlet air of the last air turbine (AT_M, state 16). It is used to heat the cold air that comes from the evaporator (E_2, state 14).
2. High grade heat stored in the remaining hot oil (HO) that is not to be used in the inter-heaters (H5).
3. Low grade heat supplied by the oil returning from inter-heaters (H6).

An ORC unit is introduced to convert the excess heat to electricity and thus increase the overall system efficiency. Three different configurations of the ORC evaporator are proposed (Fig. 2). High grade (H) uses hot oil directly from the hot oil tank (state H5) and neglects the return oil (state H6) as heat source for ORC. In the two-stage (2S) configuration, a second heat exchanger is added to preheat the ORC working fluid using low grade heat (state H6) firstly, and then hot oil (state H5) secondly. In the last configuration investigated (low grade – L), the two streams of oil – high and low grade – are mixed before entering the evaporator.

3. MATHEMATICAL MODEL

A simulation code developed in MATLAB R2023a [20] was used to predict thermodynamic state in each point of the system and to evaluate the efficiency metrics. Thermodynamic properties of air, propane, methanol and R32 were calculated using REFPROP 10.0 [21]. Properties of molten salt are based on the System Advisor Model [22], and thermal oil (*Therminol 66*) properties are based on data supplied by the manufacturer [23].

Table 2 Minimum temperature differences in heat exchangers

Heat exchanger groups	Minimum temperature difference
Cold-box (CB), evaporators (E), ORC condenser (OC)	5 K
Inter-coolers (IC), air regenerator (AR), oil inter-heaters (OIH), salt inter-heaters (SIH), ORC evaporator (OE)	10 K

Table 3 Component efficiencies

Components	Efficiency type	Efficiency value (%)
Air compressors (AC)	Polytropic	90
Air turbines (AT)	Polytropic	85
ORC turbine (OT)	Polytropic	85
Cryo-turbine (CRT)	Isentropic	70
Cryo-pump (CRP)	Isentropic	70
ORC pump (OP)	Isentropic	70
Air heat exchangers	Pressure loss	1
Motors and generators	Mechanical	100

3.1 Main assumptions

The thermodynamic model is based on the following assumptions:

1. It is a design simulation model. The components are scaled depending on conditions, to reach the design parameters.
2. Air is regarded as a mixture of nitrogen and oxygen. Ambient conditions are: 20 °C, 1 bar, nitrogen mole fraction 0.793.
3. The thermal oil is *Therminol 66 following the* recommended temperature range from -3 °C to 349 °C.

4. The molten salt is *Solar Salt* (60% $NaNO_3$, 40% KNO_3) with an approximate usable temperature range from 260 °C to 620 °C [24]. In the model the lower boundary is raised to 317 °C to accommodate for CSP operation problems closer to the freezing temperature.
5. CSP supplies as much heat as LAES demands (the heliostats field is scaled accordingly).
6. The ORC working fluid is R32 (Difluoromethane).
7. The design minimum temperature differences of the heat exchangers are listed in Table 2.
8. The efficiencies of the system components are listed in Table 3.

3.2 Energy analysis model

The power of turbomachinery and pumps is obtained from:

$$\dot{W} = \dot{m}(h_{out} - h_{in}) \quad (1)$$

where $\dot{W}$ [kW] is power, $\dot{m}$ [kg/s] is mass flow rate, h_{in} and h_{out} [kJ/kg] are inlet and outlet specific enthalpies respectively.

3.2.1 Isentropic efficiency

Outlet enthalpies of turbomachines and pumps are calculated based on isentropic efficiency. For turbines it is defined as:

$$\eta_{is}^{T} = \frac{h_{out} - h_{in}}{h_{out,is} - h_{in}} \quad (2)$$

where h_{out} is turbine outlet enthalpy, h_{in} is turbine inlet enthalpy and $h_{out,is}$ is theoretical outlet enthalpy of isentropic expansion.

For compressors and pumps it is defined as:

$$\eta_{is}^{C} = \frac{h_{out,is} - h_{in}}{h_{out} - h_{in}} \quad (3)$$

where h_{out} is compressor outlet enthalpy, h_{in} is compressor inlet enthalpy and $h_{out,is}$ is theoretical outlet enthalpy of isentropic compression.

3.2.2 Polytropic efficiency

Polytropic efficiency is used for the air compressors and turbines, as well as the ORC turbine because of the wide range of pressure ratios analyzed. For turbomachines working with air, isentropic efficiencies were obtained based on polytropic efficiencies and pressure ratios assuming ideal gas and neglecting variations of properties with temperature. The isentropic efficiency of the ORC turbine is obtained using Huntington 3-point method [25].

3.3 Efficiency indices

Charge and discharge work are defined as follows:

$$W_{ch} = \sum_{i=1}^{N} W_{AC_i} + W_{CRT} \quad (4)$$

$$W_{dis} = |\sum_{i=1}^{M} W_{AT_i} + W_{CRP} + W_{OT} + W_{OP}| \quad (5)$$

where W_{ch} [MWh] is charge work, W_{AC_i} [MWh] is energy consumption of the i-th compressor, N is a number of air compressors, W_{CRT} [MWh] is work output of the cryo-turbine, W_{dis} [MWh] is discharge work, W_{AT_i} [MWh] is the work of the i-th turbine, M is the number of air turbines, W_{CRP} [MWh] is electricity consumption of the air cryo-pump, W_{OT} is the work of ORC turbine, W_{OP} is electricity consumption of ORC pump.

The efficiency of the liquefaction process is measured with the liquid yield calculated as follows:

$$Y = \frac{\dot{m}_7}{\dot{m}_6} \quad (6)$$

The round-trip efficiency and round-trip exergy ratio are defined as:

$$RTE = \frac{W_{dis}}{W_{ch}} \quad (7)$$

$$RTE_{ex} = \frac{W_{dis}}{W_{ch} + \Delta Ex_{salt}} \quad (8)$$

$$\Delta Ex_{salt} = Ex_{S3} - Ex_{S4} \quad (9)$$

where Ex_P is the exergy of the salt in point P.

To evaluate the efficiency of SALAES discharge from the perspective of solar heat to electricity conversion (solar power cycle), a new metric, solar power cycle efficiency, η_{sol} is proposed:

$$\eta_{sol} = \frac{W_{dis}^{SALAES} - W_{dis}^{LAES}}{Q_{salt}} \quad (10)$$

$$Q_{salt} = m_{salt}(h_{S3} - h_{S4}) \quad (11)$$

where W_{dis}^{LAES} is discharge work of LAES not coupled with a CSP plant, and W_{dis}^{SALAES} is discharge work of LAES coupled with CSP plant (SALAES).

The performance of the ORC unit is evaluated using:

$$\eta_{ORC} = \frac{|W_{OT} + W_{OP}|}{Q_{evap}} \quad (12)$$

$$Q_{evap} = \dot{m}_{ORC}(h_{O2} - h_{O1})\, t_{dis} \quad (13)$$

where t_{dis} is total discharge time.

Table 4 Model verification results

System	Indices	Reference value	Simulation result	Relative deviation (%)
LAES [24]	RTE (%)	54.4	54.5	0.2
	Liquid yield (%)	84.2	84.2	<0.1
LAES-ORC [25]	RTE – base (%)	50.3	48.8	3.0
	RTE – with ORC (%)	55.5	53.8	3.1
	Liquid yield (%)	60.5	58.8	2.8
	Turbine power (MW)	47.77	46.68	2.3
	ORC power (MW)	7.1	7.09	0.1
	ORC efficiency (%)	20.15	20.26	0.5
SALAES [13]	RTE (%)	72.38	71.26	1.5
	Liquid yield (%)	85.3	82.2	3.6
	ORC efficiency (%)	13.56	12.91	4.8
	Solar salt mass flow rate (kg/s)	53.12	55.2	3.9

3.4 Model verification

The SALAES technology is yet to be demonstrated, thus the model was verified using results from other LAES analyses in the literature (Table 4). The cold-box (CB_1, CB_2) and liquefaction process were verified with the results from Guizzi et al. [26] and the relative deviations of the RTE and liquid yield are 0.2 % and below 0.1 % respectively. The ORC loop was compared to the results obtained by She et al. [27], and the models are in agreement in predicting the ORC thermal efficiency and power (maximum deviation of 0.5 %). The SALAES system was compared to results from Zhou et al. [13] with a similar system layout. The predicted solar salt consumption was on the same level (3.9 % deviation), despite some differences in the system schematic and operation.

4. RESULTS AND DISCUSSION

A series of parametric studies were conducted to select the optimum charging and discharging pressures (pressures in points 3 and 12, respectively), number of compressors and turbines, and ORC evaporator configuration for a range of hot molten salt temperatures. Firstly, the liquefaction and evaporation processes were simulated for charging pressures from 100 bar to 300 bar and discharging pressures from 40 bar to 200 bar. Consequently, a study to find the optimum number of compressors and turbines for different

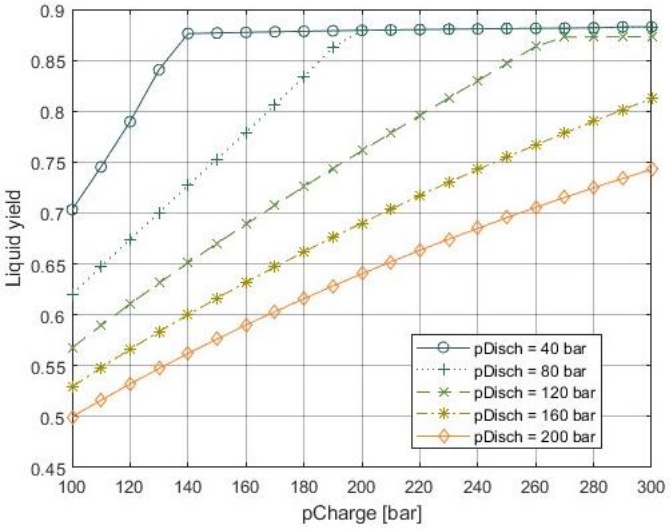

Fig. 3 Liquid air yield for different charging and discharging pressures.

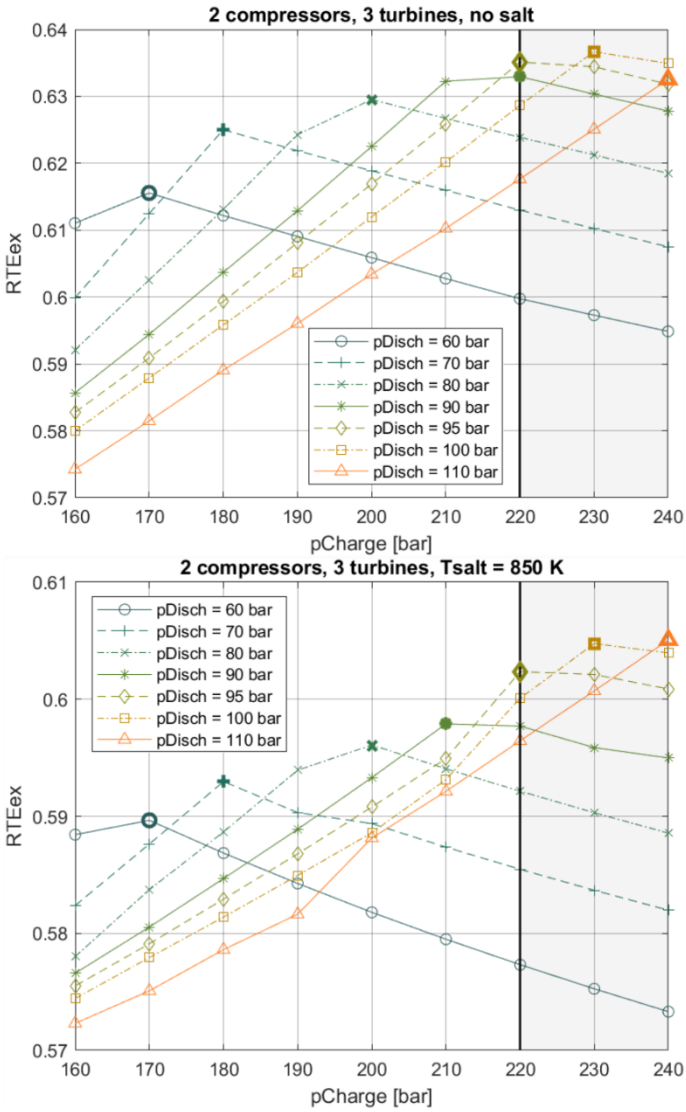

Fig. 4 Effects of charging and discharging pressures on round trip exergy ratio.

molten salt temperatures was carried out. The maximum charging pressure was restricted to 220 bar and the simulations were run only for pressures in the vicinity of the expected optimum. The number of compressors and turbines ranged from 2 to 4. Molten salt temperatures ranged from 650 K to 850 K.

4.1 Effects of charging and discharging pressures

4.1.1 Liquid yield

The results suggest that the maximum liquid yield is 88.3 %. It is mostly dependent on cold-box outlet temperature (state 5) and less on the pressure ratio in the cryo-turbine (CRT), for the given range. For every discharging pressure, the liquid yield increases with increasing charging pressure until it reaches a plateau with almost constant liquid yield (Fig. 3). The plateau starts when the cold-box outlet temperature (state 5) reaches the minimum constrained by the temperature of cold propane (state C1) and the design minimum temperature difference (cold-box pinch point is located on the cold side). After the plateau is reached, a marginal increase of liquid yield is caused only by increasing the charging pressure, because the inlet turbine temperature is constant. For higher discharge pressures the plateau is located slightly lower, because of higher cryo-pump outlet temperature (state 12) forcing the propane temperature (state C1) to increase.

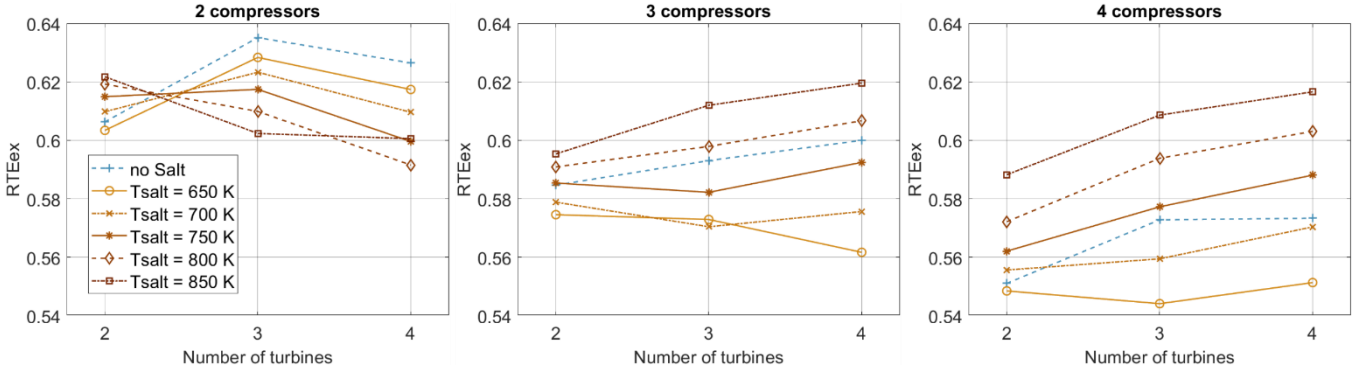

Fig. 5 Effects of molten salt temperature on the maximum round trip exergy ratio

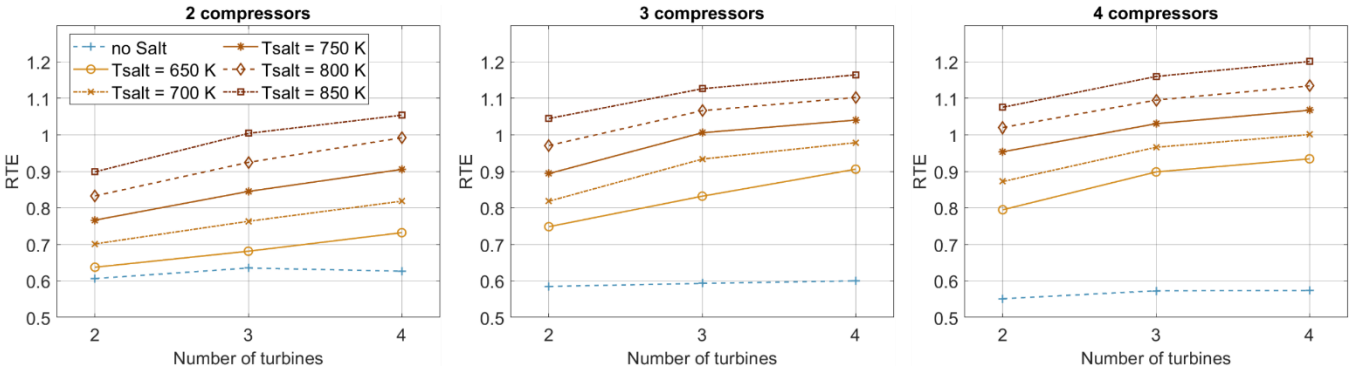

Fig. 6 Effects of molten salt temperature on round trip efficiency in points with the maximum round trip exergy ratio.

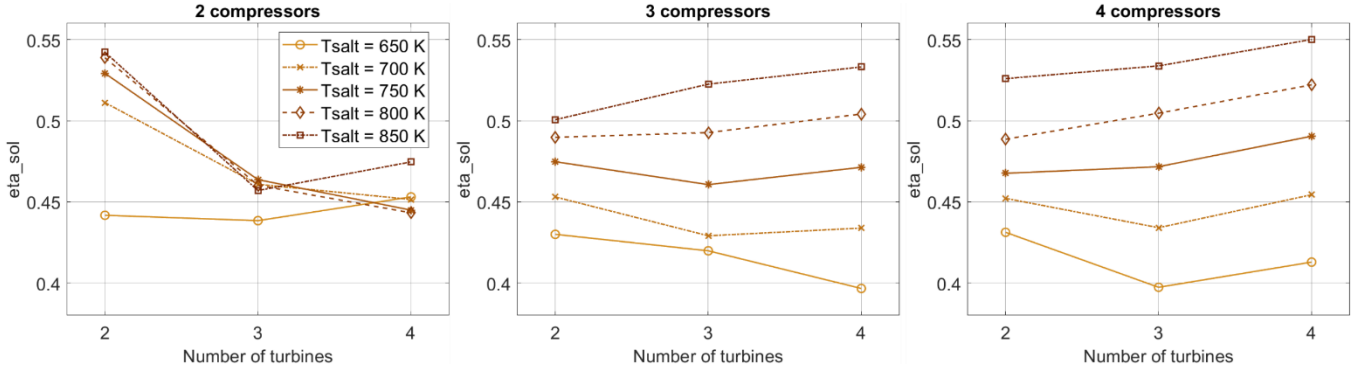

Fig. 7 Effects of molten salt temperature on solar power cycle efficiency in points with the maximum round trip exergy ratio.

4.1.2 Round trip exergy ratio

For every discharging pressure, the results indicate that the maximum RTE_{ex} is at the lowest charging pressure for which liquid yield is near the maximum (lowest charging pressure on previously described plateau). Based on that, the optimum charging pressure for the proposed system can be found in proximity to:

$$p_{ch} = 0.00187 \cdot {p_{dis}}^2 + 1.25 \cdot p_{dis} + 86.5 \qquad (14)$$

where p_{ch} and p_{dis} are given in [bar]. The equation is valid for all the analyzed cases, regardless of number of compressors and turbines and the molten salt temperature. The polynomial was obtained from curve fitting of points on liquid yield plateau with the lowest charging pressure for all considered discharge pressures.

For most investigated cases the maximum RTE_{ex} occurs for the maximum charging pressure – 220 bar, and for discharging pressure of 95 bar (Fig. 4).

4.2 Effects of molten salt temperature

4.2.1 Round-trip efficiency and round-trip exergy ratio

The effects of the molten salt temperature on RTE_{ex} are shown on Fig. 5. The results suggest that the highest RTE_{ex} for molten salt temperatures below 800 K is achieved for the system with 2 compressors and 3 turbines. This configuration is also optimal for standalone LAES (no CSP integration case). The main reason behind this is complete or almost complete utilization of hot oil in the inter-heaters, meaning that the compression heat is utilized more efficiently (less percentage of the hot oil is used by less efficient ORC). Moreover, for 2 compressors, the thermal oil is the hottest due to the highest compression ratios. It is hot enough to use the oil inter-heaters even for the highest molten salt temperatures (turbine outlets are still colder than the hot oil). The higher the molten salt temperature, the higher the RTE (Fig. 6). Increasing the number of compressors increases the solar heat consumption and the total power output for SALAES systems, however, it decreases the RTE_{ex}.

4.2.2 Solar cycle efficiency

The results indicate that the solar cycle efficiency for the cases with maximum RTE_{ex} (optimum pressures) ranges from 39.6 % to 54.2 %. In general, the solar cycle efficiency increases with increasing molten salt temperature (with a few exceptions - Fig. 7). In Fig. 8, the solar cycle efficiency range is compared with the range of design solar cycle efficiency in traditional CSP plants [28]. Even though the solar cycle efficiency cannot be considered a power cycle efficiency indicator, the comparison with steam Rankine cycle suggests that the conversion of solar heat to electricity using a SALAES system is effective.

4.2.3 Excess heat utilization

The ORC system was optimized for the maximum power output with three optimization variables: working fluid mass flow rate, evaporation pressure (from 60 bar to 150 bar) and evaporator configuration (Fig. 2). The optimal heat exchanger configuration was selected for every investigated case (Fig. 9). The choice of optimal configuration is primarily governed by the temperatures and mass flow rates of excess thermal oil (state H5 and H6). The highest power output is a trade-off between the highest ORC efficiency and the highest heat source consumption. There is a clear dependency between the molten salt temperature and the optimal ORC configuration. Starting from the lowest temperatures, configuration H is selected, because the turbine outlet temperatures are low, which lowers the quality of the low-grade heat. Even though there can be more low-grade oil than high-grade heat, it is more beneficial to discard the low temperature heat source and increase the ORC efficiency. Gradually, the temperature of the oil returning from the inter-heaters increases with the increasing molten salt temperature. Configuration L becomes the optimal one, because the temperature of the returning oil is now high enough to achieve higher ORC efficiency, and the mixed oil provides much more heat than the high temperature oil alone. Subsequently, after further increase in molten salt temperature, the turbine outlet becomes hotter than the hot oil temperature and the oil cannot take part in the inter-

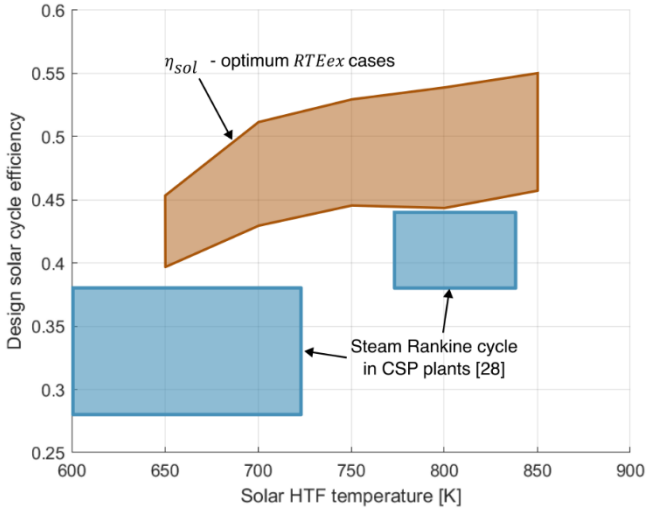

Fig. 8 Range of solar cycle efficiency for optimum RTEex cases

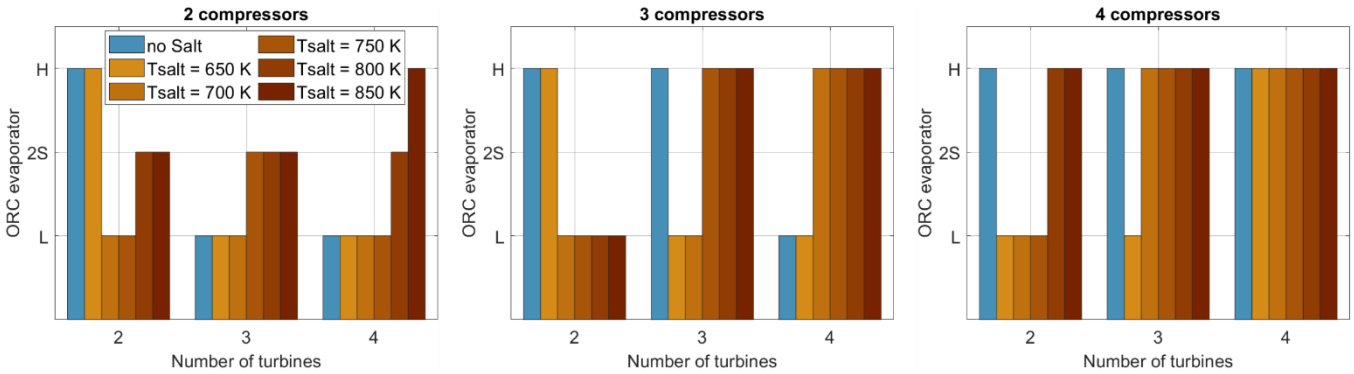

Fig. 9 Effects of molten salt temperature on the optimum ORC evaporator configuration.

heating process. This results in a higher available mass of high-grade oil and the optimum moves towards configuration H. In the transition zone, configuration 2S can be the optimal, depending on the mass flow rates and temperatures of both excess heat sources. For higher numbers of compressors, the temperature of the hot oil decreases. This accelerates the changes in just described tendencies (e.g. oil inter-heaters are already bypassed for lower molten salt temperatures).

The results indicate that ORC with evaporator configuration 2S has the highest output power in several cases. However, the RTE_{ex} of the system is on average only 0.1 % higher than that of the second-best configuration, with maximum difference of 0.2 %. The effect of changing the configuration from H to L, or vice versa on RTE_{ex} is much stronger. For the cases with the highest RTE_{ex} achieved for configuration H, the RTE_{ex} is on average 11.8 % higher than for L, with the maximum difference of 10.9 % and the minimum difference of 0.1 %. For the cases with the highest RTE_{ex} achieved for configuration L, the RTE_{ex} is on average 7 % higher than for H, with the maximum difference of 10.2 % and the minimum difference of 0.2 %.

5. CONCLUSIONS

In this paper, effects of solar heat transfer fluid (HTF) temperature on the optimal solar aided liquid air energy storage system (SALAES) layout were studied. A correlation between charging and discharging pressures was derived, to achieve round-trip exergy ratio (RTE_{ex}) close to the maximum. A new indicator – solar cycle efficiency has been proposed to measure the efficiency of solar heat to electricity conversion in SALAES systems. Three organic Rankine cycle (ORC) evaporator configurations were studied to optimize the multisource excess heat utilization. Maximum RTE_{ex} of 62.2 % is obtained for the maximum analyzed molten salt (solar HTF) temperature (850 K) and system with 2 compressors and 2 turbines. The optimum system layout is 2 compressors and 3 turbines for solar HTF temperatures below 800 K. The results indicate that the solar heat to electricity conversion efficiency of SALAES system may be higher than that of a steam Rankine cycle used in the majority of concentrated solar power plants. A clear dependency of molten salt temperature on the selection of optimum configuration is observed. The results suggest that the two-stage configuration of the ORC evaporator is the best for several cases (highest RTE_{ex} obtained). However, the improvement of RTE_{ex} in relation to second-best configuration is negligible. Based on the findings, we suggest to use one heat exchanger that is able to work in both high-grade (H) and low-grade (L) configurations in the case of systems with variable solar HTF temperature in off-design conditions (the limited amount of hot solar HTF would be then mixed with the return flow). The difference between RTE_{ex} attained from systems with H and L configurations exceeds 10 percentage points in some cases.

ACKNOWLEDGEMENT

The research presented in this paper was partly developed within the project “Sustainable large-scale energy storage in Egypt” (Project no. 21-M13-DTU), funded by the Ministry of Foreign Affairs of Denmark and administrated by Danida Fellowship Centre. The financial support is gratefully acknowledged.

REFERENCES

[1] UN: Paris agreement. 2015, U.N. Doc. FCCC/CP/2015/L.9/Rev/1

[2] REN21.2022. Renewables 2022 Global Status Report. Paris: REN21 Secretariat.

[3] Gøtske AK, Andresen GB, Victoria M. Cost and Efficiency Requirements for Successful Electricity Storage in a Highly Renewable European Energy System. PRX Energy 2, 023006 (2023).

[4] Cárdenas B, Swinfen-Styles L, Rouse J, Garvey SD. Short-, Medium-, and Long-Duration Energy Storage in a

100% Renewable Electricity Grid: A UK Case Study. Energies 2021, 14, 8524.
[5] Vecchi A, Li Y, Ding Y, Mancarella P, Sciacovelli A. Liquid air energy storage (LAES): A review on technology state-of-the-art, integration pathways and future perspectives. Advances in Applied Energy 3 (2021) 100047.
[6] Liang T, Zhang T, Lin X, Tafone A et al. Liquid air energy storage technology: a comprehensive review of research, development and deployment. Prog. Energy 5 (2023) 012002.
[7] Li D, Duan L. Design and analysis of flexible integration of solar aided liquid air energy storage system. Energy 259 (2022) 125004.
[8] Yang M, Duan L, Tong Y, Jiang Y. Study on design optimization of new liquified air energy storage (LAES) system coupled with solar energy. Journal of Energy Storage 51 (2022) 104365.
[9] Li D, Duan L. Techno-economic analysis of solar aided liquid air energy storage system with a new air compression heat utilization method. Energy Conversion and Management 278 (2023) 116729.
[10] Li D, Duan L, Ding X. New regulation strategies study of solar aided liquid air energy storage system under off-design conditions. Energy Conversion and Management 270 (2022) 116287.
[11] Ji W. Zhou Y, Sun Y, Zhang W, Pan CZ, Wan JJ. Thermodynamic characteristics of a novel wind-solar-liquid air energy storage. Materials Science and engineering 278 (2017) 012070.
[12] Nabat MH, Soltani M, Razmi AR, Nathwani J, Dusseault MB. Investigation of a green energy storage system based on liquid air energy storage (LAES) and high-temperature concentrated solar power (CSP): Energy, exergy, economic and environmental (4E) assessments, along with a case study for San Diego, US. Sustainable Cities and Society 75 (2021) 103305.
[13] Zhou Y, Duan L, Ding X, Li M, Gao C. Performance study on a new solar aided liquid air energy storage system integrated with organic Rankine cycle and thermoelectric generator. Journal of energy storage 59 (2023) 106566.
[14] Ding X, Duan L, Zhou Y, Gao C, Bao Y. Energy, exergy, and economic analyses of a new liquid air energy storage system coupled with solar heat and organic Rankine cycle. Energy Conversion and Management 266 (2022) 115828.
[15] Zhou Y, Duan L, Ding X, Bao Y, Tian F. Economic feasibility assessment of a solar aided liquid air energy storage system with different operation strategies. Journal of Energy Storage 72 (2023) 108812.
[16] Zhou Y, Duan L, Ding X, Zheng N. Dynamic performance analysis of the discharging process of a solar aided liquid air energy storage system. Journal of Energy Storage 73 (2023) 108891.
[17] Ebrahimi A, Ghorbani B, Skandarzadeh F, Ziabasharhagh M. Introducing a novel liquid air cryogenic energy storage system using phase change material, solar parabolic trough collectors, and Kalina power cycle (process integration, pinch, and exergy analyses). Energy Conversion and Management 228 (2021) 113653.
[18] Derakhshan S, Khosravian M. Exergy Optimization of a Novel Combination of a Liquid Air Energy Storage System and a Parabolic trough Solar Collector Power Plant. Journal of energy Resources Technology. Aug 2019, 141(8): 081901.
[19] Li Y, Wang X, Jin Y, Ding Y. An integrated solar-cryogen hybrid power system. Renewable Energy 37 (2012) 76-81.
[20] The MathWorks Inc. (2023). MATLAB version: 9.14.0.2306882 (R2023a) Update 4, Natick, Massachusetts: The MathWorks Inc. https://www.mathworks.com
[21] Lemmon, E.W., Bell, I.H., Huber, M.L., McLinden, M.O. NIST Standard Reference Database 23: Reference Fluid Thermodynamic and Transport Properties-REFPROP, Version 10.0, National Institute of Standards and Technology, Standard Reference Data Program, Gaithersburg, 2018.
[22] Blair N, DiOrio N, Freeman J, Gilman P et al. System Advisor Model (SAM) General Description (Version 2017.9.5). Golden, CO: National Renewable Energy Laboratory. NREL/ TP-6A20-70414.
[23] Therminol 66 heat transfer fluid technical bulletin. https://www.therminol.com/sites/therminol/files/documents/TF-8695_Therminol-66_Technical_Bulletin.pdf
[24] Zhang HL, Baeyens J, Degrève J, Cacères G. Concentrated solar power plants: Review and design methodology. Renewable and Sustainable Energy Review 22 (2013) 466-481.
[25] Huntington RA. Evaluation of Polytropic Calculation Methods for Turbomachinery Performance. Journal of engineering for Gas Turbines and Power. Oct 1985, 107(4): 872-876.
[26] Guizzi GL, Manno M, Tolomei LM, Vitali RM. Thermodynamic analysis of a liquid air energy storage system. Energy 93 (2015) 1639-1647.
[27] She X, Peng X, Nie B, Leng G, Zhang X et al. Enhancement of round trip efficiency of liquid air energy storage through effective utilization of heat of compression. Applied Energy 206 (2017) 1632-1642.
[28] He YL, Qiu Y, Wang K, Yuan F et al. Perspective of concentrating solar power. Energy 198 (2020) 117373.